

## RESEARCH ARTICLE

# Evaluation of [<sup>18</sup>F]CP18 as a Substrate-Based Apoptosis Imaging Agent for the Assessment of Early Treatment Response in Oncology

Sara Ropic,<sup>1</sup> Christel Vangestel,<sup>1,2</sup> Filipe Elvas,<sup>1,2</sup> Jeroen Verhaeghe,<sup>1</sup>  
Tim Van den Wyngaert,<sup>1,2</sup> Leonie wyffels,<sup>1,2</sup> Patrick Pauwels,<sup>3,4</sup> Steven Staelens,<sup>1</sup>  
Sigrid Stroobants<sup>1,2</sup>

<sup>1</sup>Molecular Imaging Center Antwerp (MICA), Faculty of Medicine and Health Sciences, University of Antwerp, Wilrijk, Belgium

<sup>2</sup>Department of Nuclear Medicine, Antwerp University Hospital, Edegem, Belgium

<sup>3</sup>Center for Oncological Research (CORE), Faculty of Medicine and Health Sciences, University of Antwerp, Wilrijk, Belgium

<sup>4</sup>Department of Pathology, Antwerp University Hospital, Edegem, Belgium

### Abstract

**Purpose:** The substrate-based positron emission tomography (PET) tracer [<sup>18</sup>F]CP18 is capable of detecting the activity of caspase-3/7, two key executioner proteases in the apoptosis pathway, through selective cleavage of the ligand by the activated proteases and subsequent accumulation in apoptotic cells. Using an *in vitro* and *in vivo* model of colorectal cancer (CRC), we investigated whether [<sup>18</sup>F]CP18 tracer accumulation provides a measure for apoptosis and reliably reflects early treatment response to chemotherapeutics.

**Procedures:** [<sup>18</sup>F]CP18 cell uptake was assessed in treated Colo205 cells (saline, 5-fluorouracil (5-FU), irinotecan or their combination) and correlated with caspase-3/7 activity. [<sup>18</sup>F]CP18 imaging was performed in Colo205 xenografts, starting with a baseline  $\mu$ PET/micro X-ray computed tomography ( $\mu$ CT) scan, followed by a 3-day treatment with saline ( $n = 5$ ), 5-FU (low sensitivity,  $n = 4$ ), irinotecan (high sensitivity,  $n = 5$ ), or a combination of both ( $n = 7$ ). The study was concluded with a second [<sup>18</sup>F]CP18 scan, 24 h after final treatment administration, followed by tumor removal for gamma counting (%ID/g) and for cleaved caspase-3 immunohistochemistry (apoptotic index/necrosis). Tumors were delineated on  $\mu$ CT images and, using the obtained volumes of interest, average percentage injected dose per cubic centimeter (%ID/cm<sup>3</sup>) was calculated from every  $\mu$ PET image.

**Results:** *In vitro*, [<sup>18</sup>F]CP18 cell uptake was positively correlated with caspase-3/7 activity ( $r = 0.59$ ,  $p = 0.003$ ). A drug-dependent increase in [<sup>18</sup>F]CP18 tumor uptake compared to baseline was observed in animals treated with 5-FU (+14 ± 25 %), irinotecan (+56 ± 54 %), and their combination (+158 ± 69 %,  $p = 0.002$ ). %ID/cm<sup>3</sup> showed a positive relationship with both %ID/g ( $r = 0.83$ ,  $p < 0.0001$ ) and the apoptotic index ( $r = 0.60$ ,  $p = 0.004$ ), but not with tumor necrosis ( $r = 0.22$ ,  $p = 0.36$ ).

**Conclusion:** Both our *in vitro* and *in vivo* findings have shown the ability of [<sup>18</sup>F]CP18-PET to visualize therapy-induced cancer cell apoptosis and possibly serve as a biomarker for early therapy response.

**Key Words:** [<sup>18</sup>F]CP18, PET, Apoptosis imaging, Caspase-3/7, Colorectal cancer

Electronic supplementary material The online version of this article (doi:10.1007/s11307-016-1037-7) contains supplementary material, which is available to authorized users.

Correspondence to: Sigrid Stroobants; e-mail: Sigrid.Stroobants@uza.be

## Introduction

In oncology, the continuous development of novel therapeutic agents has fueled the need for biomarkers to monitor therapy-induced changes through observation of cancer hallmarks including apoptosis. Successful anticancer treatments often result in apoptosis of cancer cells in an early phase; thus, visualizing this process non-invasively by means of positron emission tomography (PET) is a sensible approach to assess early response to anticancer therapy. Two different pathways can initiate apoptosis: the intrinsic pathway activated by cellular stress and the extrinsic pathway operating through death receptors (Fig. 1). Specific proteases called caspases regulate and activate these pathways, converging at the level of caspase-3/7, which makes caspase-3/7 activation a suitable marker for apoptosis [1].

Over the past decade, several nuclear imaging agents targeting cell death have been developed, but, so far, no apoptosis tracer has yet been approved for clinical use. The most intensively investigated and frequently used probe for cell death imaging is Annexin A5, based on its high affinity for phosphatidylserine (PS) [2, 3]. In viable cells, PS is present in the inner leaflet of the plasma membrane, but flips to the outer leaflet upon exposure of the cells to apoptotic stimuli. Therefore, PS externalization is considered a hallmark of dying cells. However, [<sup>99m</sup>Tc]Annexin A5 has shown high blood-pool activity and a strong background signal in abdominal tissues due to liver and kidney clearance, limiting the application of this probe for abdominal imaging [1, 4]. Another apoptosis imaging target is phosphatidylethanolamine (PE), which, like PS, is accessible during cell death. Duramycin is a 19-amino acid peptide that binds to PE with high affinity. Labeled with Technetium-99m, it has shown favorable pharmacokinetics and biodistribution properties [2, 3, 5] and was capable to image induction of cell death early after chemotherapy and radiotherapy as demonstrated in a mouse model of colorectal cancer [6, 7]. PE and PS imaging tracers do not exclusively target apoptotic cells, however, but also cells dying through necrosis, a passive and less regulated form of cell death, which is often a secondary and generally delayed effect after chemo- or radiotherapy [8]. Therefore, radiotracers that selectively bind activated caspase-3/7 and are thus unambiguously linked to apoptosis could have an added value to the early evaluation of therapy response. [<sup>18</sup>F]ICMT-11, an isatin-based agent, is such a caspase-3 specific probe, which has shown promise for the early detection of drug-induced tumor apoptosis in xenograft tumor models [9, 10]. Nevertheless, isatin-based agents are reported to be cleared via the hepatobiliary route, leading to an unfavorable biodistribution profile with high background liver uptake and low absolute tumor uptake [11].

The recently developed caspase-3 specific tracer [<sup>18</sup>F]CP18 is a substrate-based probe with a DEVD sequence as its key recognition element. Additionally, it has a short polyethyleneglycol (PEG) chain incorporated, resulting in better pharmacokinetic properties and enhanced cell permeability, leading to higher target tracer

uptake. Following cell penetration and recognition by intracellular activate caspase-3/7, [<sup>18</sup>F]CP18 is cleaved by the enzymes, causing a loss of the C-terminus PEG chain. The resulting polar [<sup>18</sup>F]-labeled metabolite is unable to permeate the cell membrane and therefore accumulates in the cytoplasm of apoptotic cells (Fig. 1). In cells lacking activated caspase-3/7, there is no metabolite formation and thus no preferential retention of [<sup>18</sup>F]CP18 [12]. The specificity of [<sup>18</sup>F]CP18 for caspase-3/7 was previously validated in different tumor cells in *in vitro* treatment and *in vivo* baseline studies, showing a caspase-3/7-dependent uptake in apoptotic tumor cells and a good correlation of the PET uptake data with *ex vivo* caspase-3/7 expression [13]. Furthermore, [<sup>18</sup>F]CP18 biodistribution and radiation dosimetry were evaluated in healthy human volunteers demonstrating a rapid, predominant renal clearance with reasonable dosimetry profiles. The urinary bladder wall was identified as critical organ since it received the highest radiation dose, advising frequent bladder voiding [14].

In the current study, we investigated for the first time the ability of [<sup>18</sup>F]CP18 to reflect early therapy-induced caspase-3/7 activation in a Colo205 colorectal cancer (CRC) xenograft mouse model. To elicit apoptosis, we subjected this model to treatment with 5-fluorouracil (5-FU [15]); a thymidylate synthase inhibitor with low activity in Colo205 cells, irinotecan [16]; a topoisomerase I inhibitor with high activity in Colo205 cells, or the combination of both.

## Material and Methods

### Radiotracer Preparation

The CP18 precursor was acquired from Siemens [12]. No carrier-added [<sup>18</sup>F]fluoride was produced in a Siemens Eclipse HP cyclotron by bombardment of [<sup>18</sup>O]H<sub>2</sub>O (Rotem Industries) by the <sup>18</sup>O(p,n)<sup>18</sup>F reaction. Radiosynthesis of [<sup>18</sup>F]CP18 was carried out on an automated synthesis module (Fluorsynthon III, Veenstra Instruments) specifically adapted to this radiosynthesis, as previously described [17]. Similarly to Su et al. [12], [<sup>18</sup>F]fluoropentyne was generated by adding a solution of the tosylate precursor in acetonitrile to the reaction vessel containing the anhydrous [<sup>18</sup>F]F<sup>-</sup>. The [<sup>18</sup>F]fluoropentyne was distilled from the reaction vessel into the click mixture containing the azide CP18 precursor, CuSO<sub>4</sub>, TBTA, and sodium ascorbate in acetonitrile and ethanol. The crude solution was diluted with 2 ml water, eluted through neutral alumina (Sep-Pak light, Waters), and purified by semi-preparative HPLC using a Knauer HPLC pump and a Smartline UV detector ( $\lambda = 254$  nm) in line with a Hi-Rad 1000-CD-X CdWO<sub>4</sub> scintillation detector (Scionix). After HPLC purification, the solution was sterile filtered and diluted with 0.9 % NaCl to reduce the ethanol concentration to <10 % in the final formulation. Radiochemical purity was determined by analytical

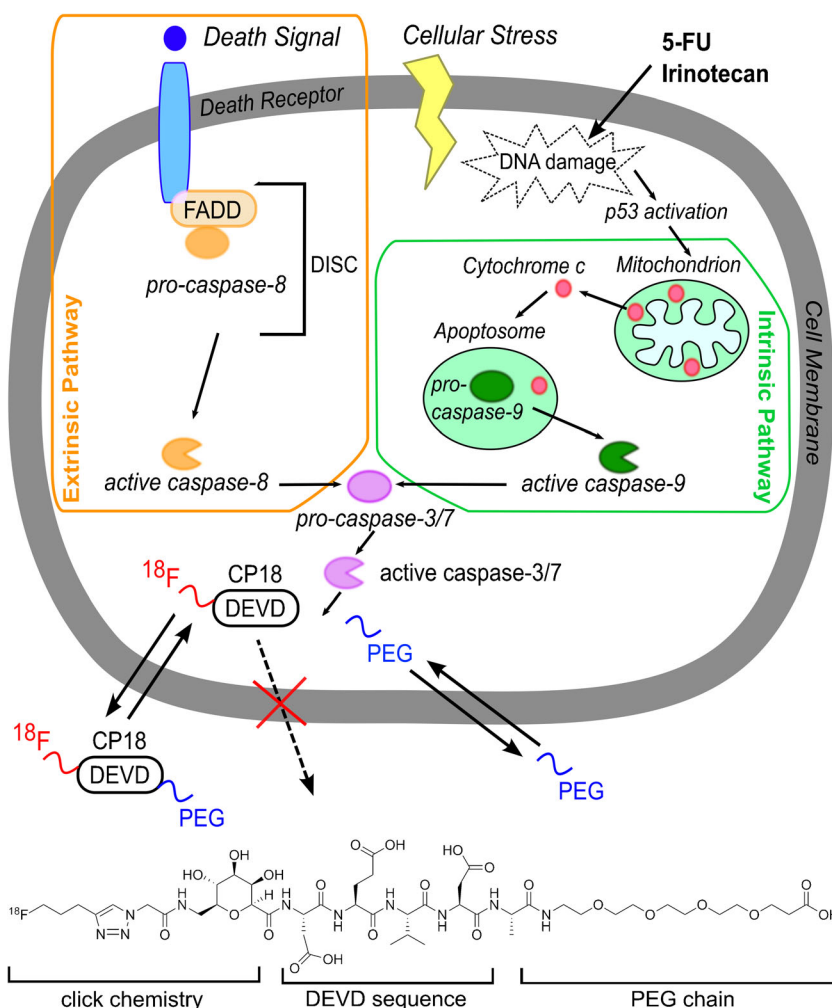


**Fig. 1** Schematic diagram of caspase-3/7 activation and [ $^{18}\text{F}$ ]CP18 uptake. The intrinsic pathway is activated by cellular stress including radio- and chemotherapy, in which case the induced DNA damage activates the tumor suppressor gene p53. Subsequent disruption of mitochondria causes the release of cytochrome c and the formation of an apoptosome, activating caspase-9. The extrinsic pathway requires the binding of extracellular apoptotic death ligands to their specific cell membrane death receptors. Ligand binding induces the formation of the DISC in the cytoplasm, activating caspase-8. Both caspase-9 and caspase-8 subsequently cleave and activate the downstream executioner caspase-3/7, ultimately leading to apoptosis. Activated caspase-3/7, in turn, is able to cleave the CP18 molecule after its DEVD sequence, separating it from its PEG chain. Consequently, metabolized [ $^{18}\text{F}$ ]CP18 is unable to cross the cell membrane and accumulates in the cytoplasm of apoptotic cells. *DEVD* amino acid sequence Asp-Glu-Val-Asp; *DISC* death-inducing signaling complex; *FADD* Fas-associated protein with death domain; *PEG* polyethyleneglycol.

reverse phase HPLC using a Shimadzu LC-20AT HPLC pump equipped with a SPD-20A UV/VIS detector ( $\lambda = 206$  nm, Shimadzu) in series with a NaI-scintillation detector for radiation detection (Raytest). The recorded data were processed by the GINA-Star 5 software (Raytest) [17]. Radiochemical yields were calculated from the theoretical initial amount of [ $^{18}\text{F}$ ]F $^-$  and decay corrected to end of bombardment.

[ $^{18}\text{F}$ ]CP18 was obtained in an average radiochemical yield of 7 % (decay corrected) with an average synthesis time of 90 min, a radiochemical purity of 99.4 %, and average specific activity of  $215 \pm 84$  GBq/ $\mu\text{mol}$  (10 syntheses).

### *In Vitro* [ $^{18}\text{F}$ ]CP18 Uptake

Semi-adherent human colon cancer cells (Colo205, PerkinElmer) were routinely cultured in RPMI 1640 culture medium supplemented with 10 % fetal bovine serum, 1 % penicillin-streptomycin, 2 mM L-glutamine, and 1 mM sodium pyruvate (all acquired from Invitrogen). Cells were maintained at 37 °C and 5 % CO $_2$ . To evaluate the uptake of [ $^{18}\text{F}$ ]CP18 in Colo205 cells,  $5 \times 10^4$  cells were seeded into six-well plates and treated with vehicle (saline,  $n = 6$  wells), clinical-grade 5-FU (0.6 mM,  $n = 6$  wells), clinical-grade irinotecan (3.4  $\mu\text{M}$ ,  $n = 6$  wells), or a combination of both chemotherapeutics ( $n = 6$  wells, same dose). Cells were

treated for 48 h after which they were incubated with [<sup>18</sup>F]-CP18 (5  $\mu$ Ci/well) at 37 °C for 1 h. After harvesting, cells were centrifuged for 5 min at 150 $\times$ g and washed twice with phosphate-buffered saline (PBS). The radioactivity in the cell pellet was measured in an automatic gamma counter (2480 Wizard<sup>2</sup>, PerkinElmer), and the number of viable cells was counted with the automated Muse™ Cell Analyzer (Merck Millipore) based on nuclear staining. Cell uptake was expressed as counts per minute (CPM) corrected for decay and cell number. Using the Muse™ Caspase-3/7 assay kit (Merck Millipore), the percentage of viable, early and late apoptotic, and necrotic cells was determined following the manufacturer's instruction.

### *In Vivo Experimental Set-Up*

All animal experiments were approved by the local ethical committee (2012-68) and were performed in accordance with European and Belgian regulation. Colo205 cells (2  $\times$  10<sup>6</sup> cells in 0.1 ml phosphate-buffered saline per mouse) were used to create subcutaneous tumors in the right hind limb of 5–7-week-old female CD1 athymic nude mice (Charles River,  $n$  = 32). Tumor diameters were measured with a digital caliper, and tumor volume was calculated as  $\frac{1}{2}$  (length  $\times$  width<sup>2</sup>). When tumors reached an average size of approximately 500 mm<sup>3</sup>, mice were randomized into four treatment groups: a vehicle group (saline,  $n$  = 8), a 5-FU-treated group (250 mg/kg of clinical-grade 50 mg/ml 5-FU,  $n$  = 8), an irinotecan-treated group (120 mg/kg clinical-grade 20 mg/ml irinotecan,  $n$  = 8), and a combination group treated first with irinotecan followed, 6 h later, by 5-FU treatment (same dose as monotherapies,  $n$  = 13). Chemotherapy doses were chosen to ensure apoptosis elicitation, as described previously [18]. All agents were administered intraperitoneally in a maximum volume of 0.2 ml, daily for three consecutive days. All animals underwent  $\mu$ PET/micro X-ray computed tomography ( $\mu$ CT) imaging before treatment starts as well as 24 h after administration of the last dose.

### *Animal Preparation*

Throughout tracer injection, tracer uptake and image acquisition, animals were maintained anesthetized with isoflurane (4 % induction, 1–2 % maintenance at 37 °C) in O<sub>2</sub>. As [<sup>18</sup>F]CP18 is predominantly cleared via the kidneys with high bladder activity as a consequence [12, 14], steps were undertaken to avoid image artifacts. In the groups treated with vehicle and the monotherapies, as well as in five animals which received the combination treatment, the radioactive urine was flushed from the animal's bladder during scan acquisition as described previously [19]. As we observed nephrotoxicity, the remaining eight animals that received a combination of both chemotherapies were instead injected subcutaneously with 0.5 mg of the diuretic furosemide (Lasix, Sanofi Aventis) 30 min prior to the

$\mu$ PET scan. Their bladder was voided manually by squeezing immediately before the scan acquisition to avoid acute post-renal obstruction due to increased kidney pressure from the mechanical flushing of the bladder. Furthermore, these mice were rehydrated daily when treatment commenced through the administration of saline via oral gavage. Despite the taken measures, some animals still exhibited affected kidney function, which could be a confounding factor in this study since the tracer is almost exclusively cleared renally. Consequently, these mice were excluded from the study, resulting in the following group sizes: vehicle group ( $n$  = 5), 5-FU group ( $n$  = 4), irinotecan group ( $n$  = 5), and combination group ( $n$  = 7). All displayed and discussed results have been obtained from these animals.

### *Image Acquisition and Analysis*

Anesthetized animals were placed onto the animal bed (Minerve), positioned in the gantry of an Inveon  $\mu$ PET/ $\mu$ CT scanner (Siemens), and a 30-min static scan was acquired 70 min after the intravenous injection of 7.4–9.25 MBq [<sup>18</sup>F]CP18.  $\mu$ PET data were reconstructed using 3-dimensional ordered subset expectation maximization (OSEM3D; 16 subsets and 2 iterations) followed by 18 maximum a posteriori (MAP) iterations including scatter and attenuation correction. This resulted in an axial field of view of 12.7 cm and a (128  $\times$  128  $\times$  159) matrix of (0.77  $\times$  0.77  $\times$  0.79) mm<sup>3</sup> voxels.  $\mu$ CT acquisitions (4 $\times$  binning mode with a 50- $\mu$ m spot size at 80 kVp and 500  $\mu$ A in 120 projections) were analytically reconstructed using the Feldkamp algorithm to a (352  $\times$  352  $\times$  606) matrix with 0.223 mm<sup>3</sup> voxels.

All analyses were performed in PMOD v3.3 (PMOD Technologies).  $\mu$ PET and  $\mu$ CT images were intrinsically co-registered since they were acquired on a multimodal gantry. Tumors were localized and delineated on the  $\mu$ CT image, defining a 3-dimensional volume of interest (VOI) encompassing the whole tumor. From the  $\mu$ PET images, the average activity (in kBq/cm<sup>3</sup>) in the tumor VOI was divided by the corresponding injected radiotracer activity (in kBq) to calculate the percentage injected dose per cubic centimeter (%ID/cm<sup>3</sup>).

### *Ex Vivo Validation*

Directly after their post-treatment scan, animals were euthanized through cervical dislocation. Tumors were removed, washed in PBS, and weighed. Tumor radioactivity was counted in an automatic gamma counter (2480 Wizard<sup>2</sup>, PerkinElmer). Uptake was decay corrected and expressed as percentage of injected dose per gram of tissue (%ID/g).

Next, tumors were fixed in formalin and embedded in paraffin. From each tumor, three central 5- $\mu$ m thick sections, each 100  $\mu$ m apart, were cut and deparaffinized in xylene and rehydrated in graded ethanol. Antigen retrieval was



performed by maintaining the sections in 10 mM citrate buffer (pH 6.0) at a sub-boiling temperature for 20 min. Endogenous peroxidase was blocked with 3 % hydrogen peroxide. Sections were stained overnight at 4 °C against cleaved caspase-3 (CC3, #9664, Cell Signaling, 1/400) followed by a 30-min incubation at room temperature with secondary goat anti-rabbit antibody (DAKO). Next, sections were treated with diaminobenzidine (10 min, DAKO), counterstained with hematoxylin (4 min, Sigma Aldrich), and mounted with water-based mounting medium (Aquatex, Merck). Whole tumor sections (three per tumor) were imaged under a light microscope (CX-31 RBSF, Olympus) at  $\times 200$  magnification. The ratio of CC3-positive cells over the total number of tumor nuclei, as well as the total percentage of necrosis were semi-automated quantified using a customized segmentation program (using Matlab and Image Processing Toolbox Release 2013a, The MathWorks Inc.) based on color thresholds and particle size.

### Statistical Analysis

All statistical analyses were performed using GraphPad Prism v6.00 (GraphPad Software). Statistical significance was set at a 5 % level ( $p \leq 0.05$ ). All data were expressed as mean  $\pm$  standard deviation (SD), unless otherwise stated. An ordinary one-way ANOVA with Dunnett's multiple comparisons test was used to compare all groups to the vehicle group. A repeated measures two-way ANOVA followed by Fisher's LSD test or Tukey's multiple comparisons test was used to compare the effect of therapy within and between groups, respectively. Correlations were determined using the Pearson correlation coefficient.

## Results

### In Vitro [<sup>18</sup>F]CP18 Uptake

[<sup>18</sup>F]CP18 uptake in the Colo205 cells (Fig. 2a) increased in a drug-dependent manner, with the lowest difference to vehicle-treated control cells in 5-FU-treated cells (fourfold increase,  $p = 0.001$ ), followed by irinotecan (fivefold increase,  $p < 0.0001$ ) and combination-treated cells (sixfold increase,  $p < 0.0001$ ). Caspase-3/7 activity was determined by distinguishing apoptotic cells from living and necrotic cells (Fig. 2b). The percentage of apoptotic cells was not different between control cells ( $10.5 \pm 2\%$ ) and 5-FU-treated cells ( $11 \pm 0.9\%$ ) yet significantly higher in cells treated with irinotecan ( $16.2 \pm 1\%$ ,  $p = 0.0003$  versus control) and with 5-FU in combination with irinotecan ( $25.4 \pm 3.3\%$ ,  $p < 0.0001$  versus control). Overall, the percentage of apoptotic cells correlated positively with [<sup>18</sup>F]CP18 cellular uptake (Fig. 2c  $r = 0.59$ ,  $p = 0.003$ ).

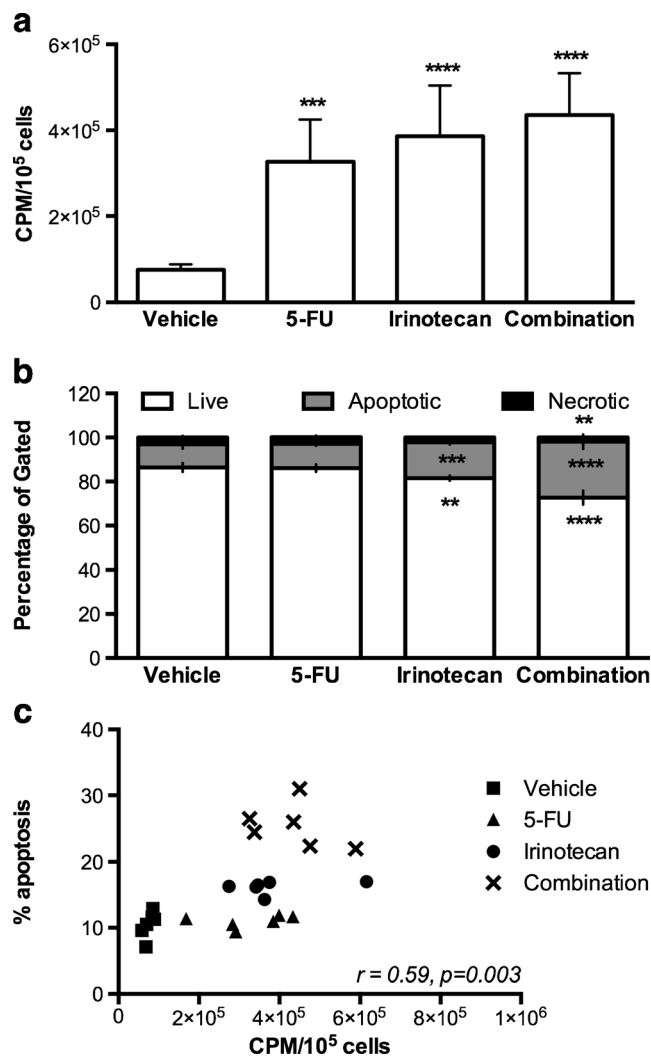


**Fig. 2** [<sup>18</sup>F]CP18 cell uptake and caspase-3/7 activation. **a** [<sup>18</sup>F]CP18 uptake in vehicle ( $n = 6$ ), 5-FU ( $n = 6$ ), irinotecan ( $n = 6$ ), and combination ( $n = 6$ )-treated cells expressed as CPM normalized to  $1 \times 10^5$  cells and compared with uptake in control vehicle-treated cells. Bars represent mean values  $\pm$  SD. \*\*\*/\*\*\* statistically significant at  $p < 0.001/p < 0.0001$ , respectively, versus vehicle. **b** Bars represent the mean percentage  $\pm$  SD of live, apoptotic, and necrotic cells after treatment with vehicle ( $n = 6$ ), 5-FU ( $n = 6$ ), irinotecan ( $n = 6$ ), or a combination of both ( $n = 6$ ). \*\*/\*\*\*/\*\*\* statistically significant at  $p < 0.01/p < 0.001/p < 0.0001$ , respectively, versus vehicle. **c** Correlation between [<sup>18</sup>F]CP18 cell uptake and the percentage of apoptotic cells ( $r = 0.59$ ,  $p = 0.003$ ).

### In Vivo [<sup>18</sup>F]CP18 Uptake

[<sup>18</sup>F]CP18 uptake was evaluated in subcutaneous Colo205 xenografts treated with either 5-FU, irinotecan, or their combination and compared with tracer uptake in the vehicle group and at baseline.  $\mu$ PET images of representative pre- and post-treatment scanned animals from each group are shown in Fig. 3a. A general lack of tracer uptake at baseline can be appreciated, and a drug-dependent, heterogeneous

increase of [<sup>18</sup>F]CP18 tumor uptake was observed after treatment. Quantified baseline [<sup>18</sup>F]CP18 uptake (Fig. 3b) was similar between all groups ( $0.34 \pm 0.11$  % ID/cm<sup>3</sup>). After treatment, %ID/cm<sup>3</sup> was insignificantly decreased in the vehicle group ( $-25 \pm 13$  %,  $p = 0.30$  versus baseline), slightly elevated in the 5-FU group ( $+14 \pm 25$  %,  $p = 0.88$  versus baseline), increased with 50 % in the irinotecan group ( $+56 \pm 54$  %,  $p = 0.46$  versus baseline), and significantly elevated with 150 % in the combination group

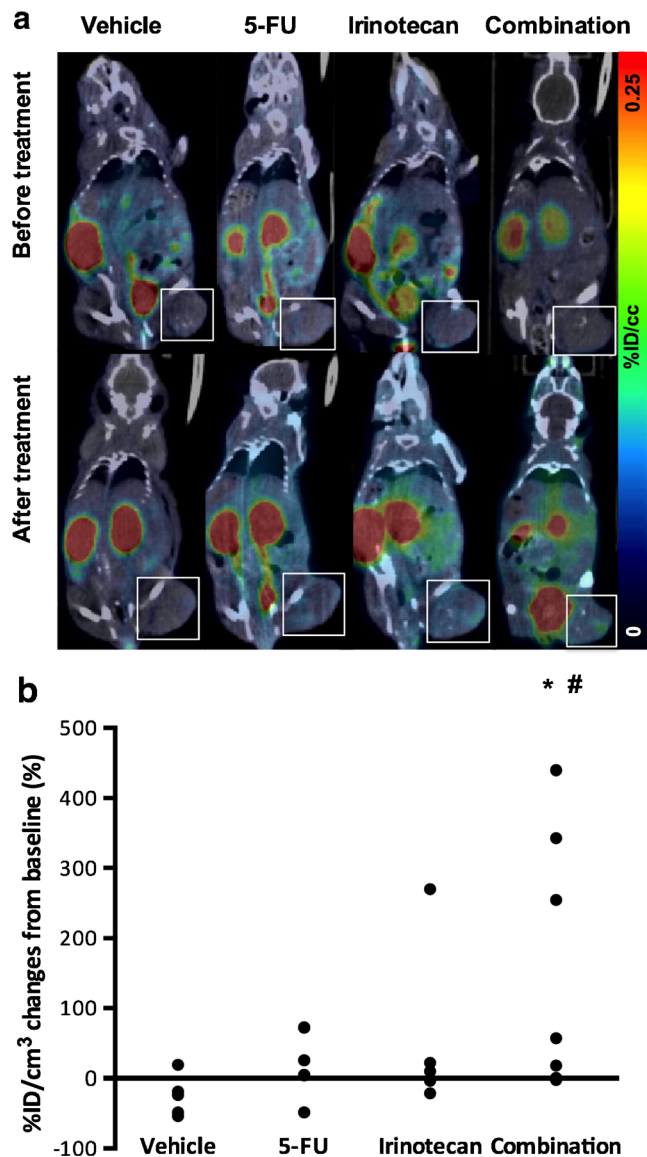


Fig. 3 *In vivo* [<sup>18</sup>F]CP18 tumor uptake. **a** Representative normalized  $\mu$ PET/CT images showing [<sup>18</sup>F]CP18 tumor uptake (%ID/cm<sup>3</sup>) in vehicle, 5-FU, irinotecan, and combination-treated animals (from left to right) before (upper panel) and after (lower panel) treatment. Tumors are indicated by white squares. **b** Plotted are the individual %ID/cm<sup>3</sup> changes (in %  $\pm$  SEM) from baseline for all vehicle ( $n = 5$ ), 5-FU ( $n = 4$ ), irinotecan ( $n = 5$ ), and combination ( $n = 7$ )-treated animals. # statistically significant at  $p < 0.01$  versus baseline, \* statistically significant at  $p < 0.01$  post-treatment versus vehicle.

( $+158 \pm 69$  %,  $p = 0.002$  versus baseline). Additionally, tumors treated with both 5-FU and irinotecan displayed a significantly higher tracer uptake compared to saline-treated tumors ( $0.60 \pm 0.32$  versus  $0.24 \pm 0.11$ %ID/cm<sup>3</sup>, respectively,  $p = 0.007$ ), while tumors treated with 5-FU ( $0.37 \pm 0.16$ %ID/cm<sup>3</sup>) or irinotecan ( $0.40 \pm 0.08$ %ID/cm<sup>3</sup>) had only a moderately elevated uptake compared with saline-treated control tumors.

### Ex Vivo Validation

Radioactivity counted in the excised tumors (in %ID/g, Fig. 4a) was found to be highest in the combination group ( $0.47 \pm 0.30$ %ID/g,  $p = 0.017$  versus control) and correlated significantly with PET uptake (in %ID/cm<sup>3</sup>, Fig. 4b  $r = 0.83$ ,  $p < 0.0001$ ). As gold standard, the level of apoptosis was evaluated using anti-CC3 immunohistochemistry in three whole tumor slices for each tumor (Fig. 5a). The apoptotic

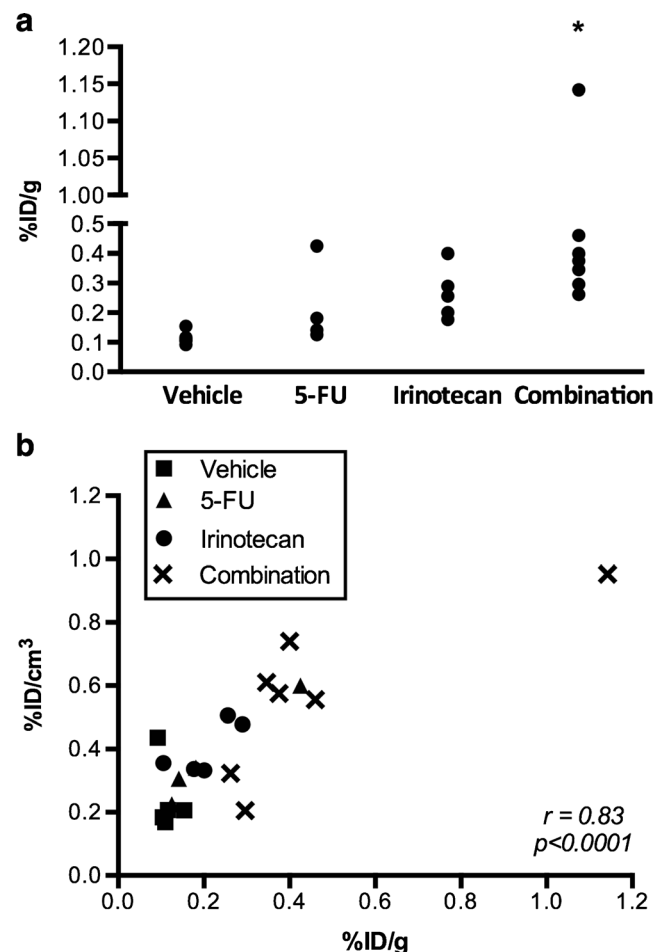


Fig. 4 *Ex vivo* [<sup>18</sup>F]CP18 tumor uptake. **a** Plotted are the individual values (%ID/g) of *ex vivo* radioactivity counted in the whole tumor of all animals treated with vehicle ( $n = 5$ ), 5-FU ( $n = 4$ ), irinotecan ( $n = 5$ ), or their combination ( $n = 7$ ). \* statistically significant at  $p < 0.05$  versus vehicle. **b** Correlation between post-treatment %ID/cm<sup>3</sup> and *ex vivo* tumor radioactivity expressed as %ID/g ( $r = 0.83$ ,  $p < 0.0001$ ).

index (Fig. 5b), determined as the ratio of apoptotic cells over nuclei, was highest in the irinotecan and combination ( $2.56 \pm 0.66$  and  $2.67 \pm 1.36$ ,  $p = 0.05$  and  $p = 0.04$  versus vehicle, respectively) treated tumors as compared with the 5-FU ( $0.59 \pm 0.25$ ) and vehicle group ( $1.42 \pm 0.72$ ). Importantly, the *in vivo* imaging data (in %ID/cm<sup>3</sup>) were moderately yet significantly correlated with the apoptotic index (Fig. 5c  $r = 0.60$ ,  $p = 0.004$ ), but not with tumor necrosis ( $r = 0.22$ ,  $p = 0.36$ ).

## Discussion

This study evaluated the ability of the novel substrate-based apoptosis PET tracer [<sup>18</sup>F]CP18 to be used as biomarker for early treatment response to chemotherapeutics using an *in vitro* and *in vivo* model of colorectal cancer. Containing the caspase-3 substrate sequence DEVD, [<sup>18</sup>F]CP18 is specifically recognized by activated caspase-3/7 and retained in the cytosol of apoptotic cells (Fig. 1). Our *in vitro* uptake study in Colo205 cells treated with vehicle, 5-FU, or irinotecan showed significantly increased [<sup>18</sup>F]CP18 cell uptake after chemotherapeutic treatment, which was overall positively correlated with caspase-3/7 activity, confirming [<sup>18</sup>F]CP18's specificity for apoptotic cells. Surprisingly, 5-FU treatment did not lead to increased caspase-3/7 activation as assessed by flow cytometry, although [<sup>18</sup>F]CP18 uptake was elevated in these cells as compared with control cells. The lack of caspase-3/7 activation could be explained by the findings from a study in which 5-FU induced caspase-9-dependent apoptosis in a CRC cell line, without the detection of other activated caspases [20]. Indeed, caspase-9 activity was significantly increased in 5-FU-treated Colo205 cells as compared with untreated controls (Supplemental Data). This would implicate, however, that the [<sup>18</sup>F]CP18 molecule is not exclusively recognized and cleaved by activated caspase-3/7. Therefore, studies with additional *in vitro* models, including drug insensitive or caspase-3/7 negative cancer cells, and studies using a radiolabeled probe with a scrambled DEVD sequence are warranted to evaluate [<sup>18</sup>F]CP18's target specificity.

In a xenograft model of CRC, we performed, to the best of our knowledge, the first preclinical study with [<sup>18</sup>F]CP18 in a tumor model with chemotherapy-induced apoptosis. So far, [<sup>18</sup>F]CP18 has only been evaluated in a dexamethasone-induced thymic apoptosis mouse model [12], in various untreated mouse xenograft tumors [13] and in a mouse model of anthracycline cardiotoxicity [21]. All studies observed a positive correlation between [<sup>18</sup>F]CP18 uptake and caspase-3/7 activity, supporting the use of [<sup>18</sup>F]CP18 for apoptosis imaging. In our study, significantly enhanced retention of [<sup>18</sup>F]CP18 was detected in tumors of animals treated with 5-FU combined with irinotecan as compared with its own baseline and with saline treated control mice. When compared to baseline uptake, an overall drug-dependent increase in post-

treatment [<sup>18</sup>F]CP18 tumor retention of approximately 15 %, 50 % and 150 % was observed in the 5-FU, irinotecan and combination group, respectively. These results correlated well with *ex vivo* radioactivity in the tumor, expressed as %ID/g.

Both *in vitro* and *in vivo*, the combination of irinotecan and 5-FU elicited the highest [<sup>18</sup>F]CP18 retention early after therapy administration, which was not surprising as these two apoptosis-inducing chemotherapies are typically administered together in the clinic to treat metastatic CRC, known as the treatment regimen FOLFIRI [22]. It has also been shown in human colon carcinoma and human head and neck squamous cell carcinoma xenografts, that pre-treatment with irinotecan, similar to our treatment protocol, achieved optimal therapeutic synergy between 5-FU and irinotecan [23]. As monotherapy, however, 5-FU had little effect on tumor apoptosis as depicted by the minor increase in our tumor uptake data. This can be explained by the Colo205 cell line's low expression level of thymidylate synthase (TS), an enzyme involved in DNA synthesis. Acting as an inhibitor of TS, 5-FU chemotherapy has demonstrated significant improvement in disease-free and overall survival for patients with high tumor TS levels [24], but has low activity in the Colo205 cell line [25]. Irinotecan monotherapy, on the other hand, has been shown to induce apoptosis in both irinotecan treated Colo205 cells [7] and xenografts [6], which we were able to detect in our study with [<sup>18</sup>F]CP18.

It is worth noting that the applied treatment regimens, based on a previous study [18] and specifically selected to elicit apoptosis, lead to weight loss which reached our ethical endpoint at day 3 when animals were accordingly scanned and euthanized. Despite rehydration, some animals suffered from chemotherapy induced nephrotoxicity [26] and were consequently excluded from the study. Flushing their bladder routinely during scan acquisition to avoid image artifacts due to spillover from the radioactive urine, seemed to exert additional stress onto the kidneys (Supplemental Data), urging caution when combining this procedure with a radiotracer that is almost exclusively cleared via the kidneys, such as [<sup>18</sup>F]CP18. Avoiding this procedure could be done by inoculating tumor cells at sites further away from the bladder, such as the shoulder or neck regions. Not only bladder flushing but also therapeutic interventions inducing nephrotoxicity may influence the pharmacokinetic profile of this radiotracer substantially, for instance through prolonged circulation times and increase data variability. Although this limitation could potentially hamper [<sup>18</sup>F]CP18's clinical application, current hydration protocols, chemotherapeutic dosage levels, and advances in the development of chemotherapeutic agents have restrained chemotherapy-induced nephrotoxicity [27].

A potential limitation of our study could be the lack of *a priori* determination of the optimal post-treatment imaging window. This knowledge concerns all apoptosis imaging

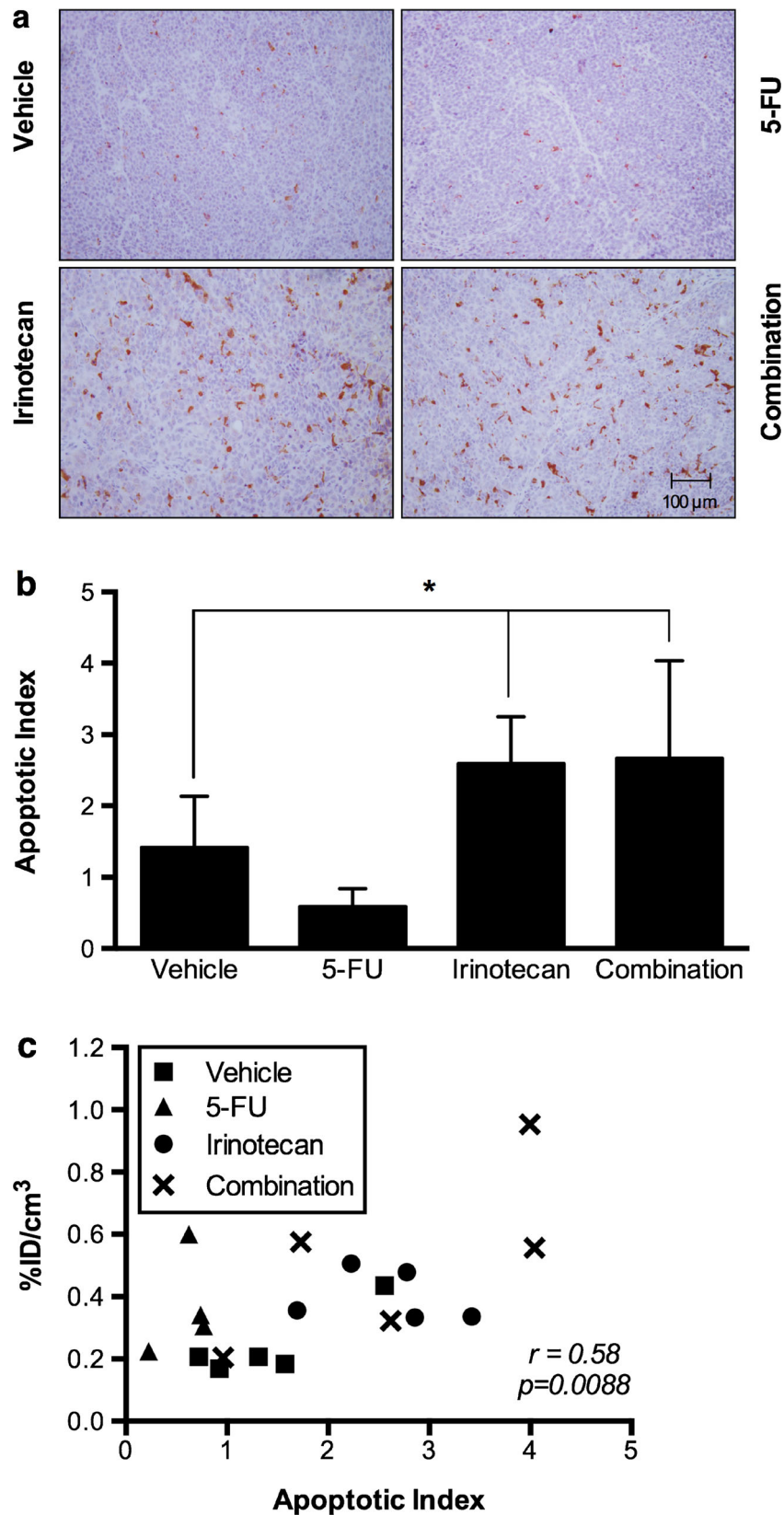


**Fig. 5** Immunohistochemical validation of imaging data. **a** Photographs ( $\times 200$ ) of representative slides from CC3 stained tumor treated with vehicle (*upper left*), 5-FU (*upper right*), irinotecan (*lower left*), or their combination (*lower right*). Positively stained tumor cells are colored *brown*. **b** Bars represent mean apoptotic index  $\pm$  SD of tumors from animals treated with vehicle ( $n = 5$ ), 5-FU ( $n = 4$ ), irinotecan ( $n = 5$ ), or their combination ( $n = 7$ ). \* statistically significant at  $p < 0.05$  versus vehicle. **c** Correlation between post-treatment %ID/cm<sup>3</sup> and CC3 in the tumor expressed as apoptotic index ( $r = 0.60$ ,  $p = 0.004$ ).



radiotracers that rely on the activation of cleaved effector caspases, due to the transient nature of this dynamic process and consequent temporal availability of the imaging target, apoptotic cells [11]. As a consequence, uptake levels in apoptotic processes are typically very low. Our averaged %ID/cm<sup>3</sup> values and changes to baseline were of the same magnitude as published in other reports of caspase-3/7 activity imaging in oncology [2, 9, 28, 29], indicating the validity of our chosen imaging window 24 h after treatment. Although only subtle differences in [<sup>18</sup>F]CP18 uptake were observed, with a doubling of tracer retention from baseline in tumors treated with the combination of 5-FU and irinotecan, the significance of this change could be determined by means of simplified, clinically feasible quantification as expressed by the averaged activity in the tumor VOI. This was in contrast to a report on [<sup>18</sup>F]ICMT-11 uptake in preclinical models of NSCLC with varying responses to carboplatin [9]. In order to detect differences in tracer uptake, the authors quantified their  $\mu$ PET data using a more complex, voxel-based analysis method, which calculated the average over the voxels exceeding the 95th percentile of the intensity in the tumor VOI.

Finally, we aimed to validate whether *in vivo* [<sup>18</sup>F]CP18 imaging correctly reflects therapy effect on tumor cell apoptosis through immunohistochemical staining against cleaved caspase-3 (apoptotic index). These results established a positive and significant correlation between post-treatment %ID/cm<sup>3</sup> and the apoptotic index, suggesting that our *in vivo* [<sup>18</sup>F]CP18 quantification accurately reflects the actual tracer uptake in the tumor. Similarly to our *in vitro* observations, no significant increase in caspase-3 activation was detected following 5-FU treatment, although [<sup>18</sup>F]CP18 tumor uptake was elevated in this group. As previously described, we hypothesize the lack of caspase-3 activation to be the consequence of 5-FU-induced caspase-9-dependent apoptosis (without the presence of other activated caspases), which is in line with observations made by Mhaidat et al. [20]. This would, however, hold implications regarding [<sup>18</sup>F]CP18's target specificity and warrants further investigations. Finally, the percentage of necrosis was determined and showed no correlation with %ID/cm<sup>3</sup>, supporting [<sup>18</sup>F]CP18 as a specific agent for apoptosis. Nevertheless, when assessing therapeutic efficacy, it could be of interest to take necrosis into consideration because it, too, is a marker of anticancer therapy response, either as a primary or secondary mechanism for tumor cell death [30], albeit typically occurring later in cell death pathways. In this case, alternative imaging approaches would be required to monitor (prolonged) treatment response. In the current study, however, it was our intention to investigate [<sup>18</sup>F]CP18's ability to assess early apoptotic response after initiation of anticancer therapy. Taken together, our findings support the use of [<sup>18</sup>F]CP18 as a potential imaging biomarker for the assessment of early apoptotic response after anticancer therapy.

## Conclusion

In a CRC *in vitro* and *in vivo* model, we have shown the ability of [<sup>18</sup>F]CP18-PET to detect early treatment response to apoptosis-inducing anticancer therapy. In treated cells, increased [<sup>18</sup>F]CP18 uptake correlated positively with caspase-3/7 activity, yet 5-FU treatment induced caspase-9-dependent apoptosis, holding implications regarding [<sup>18</sup>F]CP18's target specificity. In xenografts, a significant increase of [<sup>18</sup>F]CP18 tumor uptake was detectable 24 h after irinotecan and 5-FU combination therapy, which correlated positively with increased tumor cell cleaved caspase-3 as assessed by immunohistochemistry. Therefore, we conclude that [<sup>18</sup>F]CP18-PET is able to visualize therapy-induced cancer cell apoptosis and can possibly serve as a biomarker for early therapy response.

**Acknowledgements.** The authors thank Philippe Joye and Caroline Berghmans of the Molecular Imaging Center Antwerp for their valuable technical assistance.

This work was funded by the University of Antwerp through a Bijzonder Onderzoeksfonds (BOF27327) for S.R. and a Geconcentreerde Onderzoeksactie (GOA G.0135.13) for F.E. Si. S and C.V. are supported by the Innovative Medicines Initiative Joint Undertaking ([www.imi.europa.eu](http://www.imi.europa.eu)) under grant agreement number 115151, resources of which are composed of financial contribution from the European Union's Seventh Framework Program (FP7/2007-2013) and EFPIA companies' in kind contribution.

## Compliance with Ethical Standards

### Conflict of Interest

The authors declare that they have no conflict of interest.

## References

1. Elmore S (2007) Apoptosis: a review of programmed cell death. *Toxicol Pathol* 35:495–516
2. Vangestel C, Peeters M, Oltenfreiter R et al (2010) *In vitro* and *in vivo* evaluation of [<sup>99m</sup>Tc]-labeled tricarbonyl His-annexin A5 as an imaging agent for the detection of phosphatidylserine-expressing cells. *Nucl Med Biol* 37:965–975
3. Blankenberg FG (2008) Monitoring of treatment-induced apoptosis in oncology with PET and SPECT. *Curr Pharm Des* 14:2974–2982
4. Reutelingsperger CPM, Dumont E, Thimister PW et al (2002) Visualization of cell death *in vivo* with the annexin A5 imaging protocol. *J Immunol Methods* 265:123–132
5. Zhao M, Li Z (2012) A single-step kit formulation for the 99m Tc-labeling of HYNIC-Duramycin. *Nucl Med Biol* 39:1006–1011
6. Elvas F, Vangestel C, Pak K et al (2016) Early prediction of tumor response to treatment: preclinical validation of 99mTc-Duramycin. *J Nucl Med* 57:805–811
7. Elvas F, Vangestel C, Rapic S et al (2015) Characterization of [<sup>99m</sup>Tc]Duramycin as a SPECT imaging agent for early assessment of tumor apoptosis. *Mol Imaging Biol* 17:838–847
8. Silva MT (2010) Secondary necrosis: the natural outcome of the complete apoptotic program. *FEBS Lett* 584:4491–4499
9. Witney TH, Fortt RR, Aboagye EO (2014) Preclinical assessment of carboplatin treatment efficacy in lung cancer by 18F-ICMT-11-positron emission tomography. *PLoS One* 9:e91694
10. Nguyen Q-D, Smith G, Glaser M et al (2009) Positron emission tomography imaging of drug-induced tumor apoptosis with a caspase-3/7 specific [<sup>18</sup>F]-labeled isatin sulfonamide. *Proc Natl Acad Sci U S A* 106:16375–16380

11. Nguyen QD, Lavdas I, Gubbins J et al (2013) Temporal and spatial evolution of therapy-induced tumor apoptosis detected by caspase-3-selective molecular imaging. *Clin Cancer Res* 19:3914–3924
12. Su H, Chen G, Gangadharmath U et al (2013) Evaluation of [<sup>18</sup>F]-CP18 as a PET imaging tracer for apoptosis. *Mol Imaging Biol* 15:739–747
13. Xia C-F, Chen G, Gangadharmath U et al (2013) *In Vitro* and *In Vivo* evaluation of the caspase-3 substrate-based radiotracer [<sup>18</sup>F]-CP18 for PET imaging of apoptosis in tumors. *Mol Imaging Biol* 15:748–757
14. Doss M, Kolb HC, Walsh JC et al (2013) Biodistribution and radiation dosimetry of <sup>18</sup>F-CP-18, a potential apoptosis imaging agent, as determined from PET/CT scans in healthy volunteers. *J Nucl Med* 54:2087–2092
15. Longley DB, Harkin DP, Johnston PG (2003) 5-fluorouracil: mechanisms of action and clinical strategies. *Nat Rev Cancer* 3:330–338
16. Rothenberg ML (2001) Irinotecan (CPT-11): recent developments and future directions—colorectal cancer and beyond. *Oncologist* 6:66–80
17. Wyffels L, Thomae D, Waldron A-M et al (2014) *In vivo* evaluation of <sup>18</sup>F-labeled TCO for pre-targeted PET imaging in the brain. *Nucl Med Biol* 41:513–523. doi:10.1016/j.nucmedbio.2014.03.023
18. Vangestel C, Van de Wiele C, Mees G et al (2012) Single-photon emission computed tomographic imaging of the early time course of therapy-induced cell death using technetium 99m tricarbonyl His-annexin A5 in a colorectal cancer xenograft model. *Mol Imaging* 11:135–147
19. Deleye S, Heylen M, Deiteren A et al (2014) Continuous flushing of the bladder in rodents reduces artifacts and improves quantification in molecular imaging. *Mol Imaging* 13:1–12
20. Mhaidat NM, Bouklihacene M (2014) 5-Fluorouracil-induced apoptosis in colorectal cancer cells is caspase-9-dependent and mediated by activation of protein kinase C-δ. *Oncol Lett* 8:699–704
21. Su H, Gorodny N, Gomez LF et al (2015) Noninvasive molecular imaging of apoptosis in a mouse model of anthracycline-induced cardiotoxicity. *Circ Cardiovasc Imaging* 8:e001952–e001952
22. Douillard JY, Cunningham D, Roth AD et al (2000) Irinotecan combined with fluorouracil compared with fluorouracil alone as first-line treatment for metastatic colorectal cancer: a multicentre randomised trial. *Lancet* 355:1041–1047
23. Azrak RG, Cao S, Slocum HK et al (2004) Therapeutic synergy between irinotecan and 5-fluorouracil against human tumor xenografts. *Clin Cancer Res* 10:1121–1129
24. Johnston PG, Fisher ER, Rockette HE et al (1994) The role of thymidylate synthase expression in prognosis and outcome of adjuvant chemotherapy in patients with rectal cancer. *J Clin Oncol* 12:2640–2647
25. Derenzini M, Montanaro L, Chilla A et al (2002) Evaluation of thymidylate synthase protein expression by Western blotting and immunohistochemistry on human colon carcinoma xenografts in nude mice. *J Histochem Cytochem* 50:1633–1640
26. de Jonge MJA, Verweij J (2006) Renal toxicities of chemotherapy. *Semin Oncol* 33:68–73
27. Lameire N (2007) The kidney in oncology. *Acta Clin Belg* 62:141–154
28. Chen DL, Engle JT, Griffin EA et al (2014) Imaging caspase-3 activation as a marker of apoptosis-targeted treatment response in cancer. *Mol Imaging Biol* 17:384–393
29. Hight MR, Cheung YY, Nickels ML et al (2014) A peptide-based positron emission tomography probe for *in vivo* detection of caspase activity in apoptotic cells. *Clin Cancer Res* 20:2126–2135
30. Krysko DV, D'Herde K, Vandenaebelle P (2006) Clearance of apoptotic and necrotic cells and its immunological consequences. *Apoptosis* 11:1709–1726